

**AFRL-SN-RS-TR-2006-208**  
**Final Technical Report**  
**June 2006**



# **PHOTONIC ARBITRARY WAVEFORM GENERATION TECHNOLOGY**

**University of Central Florida**

*APPROVED FOR PUBLIC RELEASE; DISTRIBUTION UNLIMITED.*

**AIR FORCE RESEARCH LABORATORY  
SENSORS DIRECTORATE  
ROME RESEARCH SITE  
ROME, NEW YORK**

## **STINFO FINAL REPORT**

This report has been reviewed by the Air Force Research Laboratory, Information Directorate, Public Affairs Office (IFOIPA) and is releasable to the National Technical Information Service (NTIS). At NTIS it will be releasable to the general public, including foreign nations.

AFRL-SN-RS-TR-2006-208 has been reviewed and is approved for publication

APPROVED:     /s/

JAMES R. HUNTER  
Project Engineer

FOR THE DIRECTOR:     /s/

RICHARD G. SHAUGHNESSY  
Chief, Rome Operations Office  
Sensors Directorate

REPORT DOCUMENTATION PAGE			Form Approved OMB No. 074-0188	
Public reporting burden for this collection of information is estimated to average 1 hour per response, including the time for reviewing instructions, searching existing data sources, gathering and maintaining the data needed, and completing and reviewing this collection of information. Send comments regarding this burden estimate or any other aspect of this collection of information, including suggestions for reducing this burden to Washington Headquarters Services, Directorate for Information Operations and Reports, 1215 Jefferson Davis Highway, Suite 1204, Arlington, VA 22202-4302, and to the Office of Management and Budget, Paperwork Reduction Project (0704-0188), Washington, DC 20503				
1. AGENCY USE ONLY (Leave blank)	2. REPORT DATE JUNE 2006	3. REPORT TYPE AND DATES COVERED Final Feb 05 – Feb 06		
4. TITLE AND SUBTITLE PHOTONIC ARBITRARY WAVEFORM GENERATION TECHNOLOGY		5. FUNDING NUMBERS C - FA8750-05-1-0068 PE - 62204F PR - AWGD TA - SN WU - 02		
6. AUTHOR(S) Peter J. Delfyett, Jr.				
7. PERFORMING ORGANIZATION NAME(S) AND ADDRESS(ES) University of Central Florida 12443 Research Parkway, Suite 207 Orlando Florida 32826-0150		8. PERFORMING ORGANIZATION REPORT NUMBER  N/A		
9. SPONSORING / MONITORING AGENCY NAME(S) AND ADDRESS(ES) Air Force Research Laboratory/SNDP 26 Electronic Parkway Rome New York 13441-4514		10. SPONSORING / MONITORING AGENCY REPORT NUMBER  AFRL-SN-RS-TR-2006-208		
11. SUPPLEMENTARY NOTES  AFRL Project Engineer: James R. Hunter/SNDP James.Hunter@rl.af.mil				
12a. DISTRIBUTION / AVAILABILITY STATEMENT  APPROVED FOR PUBLIC RELEASE; DISTRIBUTION UNLIMITED. PA #06-416			12b. DISTRIBUTION CODE	
13. ABSTRACT (Maximum 200 Words) Modelocked semiconductor lasers emit short (<1 picosecond) optical pulses at high pulse repetition frequencies (> 1 GHz) and can be utilized for a wide variety of applications, but are typically geared towards time domain applications, e.g., optical time division multiplexed optical links, optical sampling, etc. Additionally, the periodic nature of optical pulse generation from modelocked semiconductor diode lasers also makes these devices ideal candidates for the generation of high quality optical frequency combs, or multiple wavelengths, in addition to the ultra short temporally stable, high peak intensity optical pulses that one is accustomed to. Modelocked semiconductor lasers are used to generate a set of phase locked optical frequencies on a periodic grid. The periodic and phase coherent nature of the optical frequency combs make it possible for the realization of high performance optical and RF arbitrary waveform synthesis. The resulting optical frequency components can be used for communication applications relying on direct detection, dense WDM, coherent detection WDM, OTDM, and OCDMA. This report highlights recent results in the use of optical frequency combs generated from semiconductors for optical and RF arbitrary waveform generation.				
14. SUBJECT TERMS Photonic waveform generation, optical waveform generation, optical synthesis, ultrafast optical waveforms, optical signal generation			15. NUMBER OF PAGES 37	
			16. PRICE CODE	
17. SECURITY CLASSIFICATION OF REPORT  UNCLASSIFIED	18. SECURITY CLASSIFICATION OF THIS PAGE  UNCLASSIFIED	19. SECURITY CLASSIFICATION OF ABSTRACT  UNCLASSIFIED	20. LIMITATION OF ABSTRACT  UL	

## Table of Contents

Executive Summary .....	1
Technical Discussion .....	2
Introduction.....	2
Theory .....	4
Simulation of Test Waveforms .....	7
Experiments .....	15
Conclusions.....	27
Recommendations.....	27
<u>References</u> .....	28

## List of Figures

Figure 1 Use of optical frequency combs for time domain, frequency domain, and code domain modulation formats .....	3
Figure 2 Chip scale optical waveform generator and waveform detector based on optical spectral synthesis .....	4
Figure 3 Time and frequency representation of a modelocked optical pulse train and waveform generation by spectral filtering .....	5
Figure 4 Schematic of the process of waveform generation based on dynamic spectral modulation .....	6
Figure 5 Concept of serrodyne modulation. (a) Experimental configuration and mathematical representation, (b) Experimental results showing the original tone and the shifted tone with spurs due to the finite fall time of the phase modulator.....	8
Figure 6 Use of two frequency comb sets in a time domain interleaving configuration for the suppression of spurs .....	9
Figure 7 Timing diagram of the applied signals to individual comb components to generate a single arbitrary tone, using time domain interleaving for spur suppression....	10
Figure 8 Simulated plots of the generated waveform for the arbitrary single tone timing diagram in Figure 7 .....	11
Figure 9 Timing diagram of the applied signals to individual comb components to generate an arbitrary tone signal .....	12

Figure 10 Simulated plots of the generated waveform for the arbitrary two tone timing diagram in Figure 9 .....	12
Figure 11 Timing diagram of the applied signals to individual comb components to generate a chirped signal.....	13
Figure 12 Simulated plots of the generated waveform for the chirp timing diagram in Figure 11 .....	14
Figure 13 Simulated plots of a generated waveform using both pulse shaping and dynamic modulation schemes to generate a ‘step-like’ transition on a carrier frequency	15
Figure 14 Schematic of a harmonically modelocked ring laser using an intracavity etalon to select a single longitudinal mode group and suppress supermode noise competition..	16
Figure 15 Output characteristics of the frequency stabilized harmonically modelocked laser. (a) Optical frequency comb, (b) intensity autocorrelation, (c) heterodyne beat measurement showing the frequency drift of the stabilized comb, and (d) the residual phase noise plot, along with the integrated timing jitter values.....	17
Figure 16 Overlaid spectral plots of the individual channels of the frequency demultiplexer pair .....	18
Figure 17 Experimental configuration of the arbitrary waveform generator.....	19
Figure 18 RF beat notes generated by selected individual optical comb components ....	19
Figure 19 Experimental results of dynamic modulation, showing the generation of RF bursts, and arbitrary RF tones, using serrodyning and time domain interleaving .....	20
Figure 20 Modulated sine waves and their corresponding RF spectra .....	21
Figure 21 Experimentally measured RF chirp spectrum (a) and its time domain counterpart. (b,c) simulations of the spectral and temporal output respectively .....	22
Figure 22 Schematic illustration of the use of optical frequency combs and injection locking to realize a coherent OCDMA receiver .....	23
Figure 23 Experimental setup demonstrating the use of optical frequency combs, injection locking and coherent detection for both analog and digital modulation formats .....	23
Figure 24 (a) Output spectra of the hybrid modelocked transmitter laser (master), (b) output spectra of the passive modelocked laser (slave), (c) selected two tones from the master laser, (d) injection locked slave laser .....	24

Figure 25 Locking dynamics of the injection locked passive modelocked laser. (a) Series of spectra for increasing injection power, (b) series of spectra showing the locking range (fixed detuning and increasing injection power) ..... 25

Figure 26 Experimental results using the injection locked combs as a coherent receiver. (a-c) two-tone analog modulation. (d-e) 223-1 PRBS digital modulation..... 26

---

## **Executive Summary**

The overall goal of this program is to utilize stabilized optical frequency combs from a modelocked diode laser as an orthogonal basis set of functions to realize an optical and/or RF arbitrary waveform generator. Applications relate to advance radar/lidar, optical communications, and signal processing.

### **Our key achievements are as follows:**

- Frequency domain based architecture using ‘comb-by-comb control’
- Architecture for spur suppression
- Timing diagrams for a variety of waveforms
- Demonstration of arbitrary RF sine waves
- Demonstration of RF chirp generation
- Comb stabilization
- Utilization of novel hyperfine filter technology

## **Technical Discussion**

### **Introduction**

The development of high speed communications interconnects and signal processing is critical for an information based economy. Lightwave technologies offer the promise of high bandwidth connectivity from component development that is manufacturable, cost effective, and electrically efficient. Most recently, the concept of optical frequency/wavelength division multiplexing has revolutionized methods of optical communications; however the development of optical systems using 100's of wavelengths present challenges for network planners. The development of compact, efficient optical sources capable of generating a multiplicity of optical frequencies/wavelength channels from a single device could potentially simplify the operation and management of high capacity optical interconnects and links. In addition, the potential for exploiting the coherent nature of light opens the possibility for spectrally efficient communications and signal processing [1,2].

Modelocked semiconductor lasers emit short ( $<1$  picosecond) optical pulses at high pulse repetition frequencies ( $> 1$  GHz) and can be utilized for a wide variety of applications, but are typically geared towards time domain applications, e.g., optical time division multiplexed optical links, optical sampling, etc. It is interesting to note that the periodic nature of optical pulse generation from modelocked semiconductor diode lasers also makes these devices ideal candidates for the generation of high quality optical frequency combs, or multiple wavelengths, in addition to the ultra short temporally stable, high peak intensity optical pulses that one is accustomed to. The optical frequency combs enables a variety of optical communication and signal processing applications that can exploit the large bandwidth and speed that picosecond pulse generation implies, however the aggregate speed and bandwidth can be achieved by spectrally channelizing the bandwidth, and utilize lower speed electronics for control of the individual spectral components of the modelocked laser. This report will highlight recent results in using modelocked semiconductor lasers for applications in networking, instrumentation and signal processing.

An example of the flexibility and utility of modelocked optical pulses/optical frequency combs in ultrahigh capacity communications and signal processing is shown in Figure 1. This figure shows 3 possibilities of how optical frequency combs can be used in: 1) analog or digital wavelength division multiplexed formats, where each comb line is independently modulated and coherently detected using combs from a separate synchronized receiver modelocked laser, 2) ultrahigh speed optical time division multiplexed formats, where the high data rate pulse sequences are temporally demultiplexed by the synchronized receiver modelocked laser and 3) optical code division multiplexed formats, where the transmitted pulses are modulated using on-off keying, and subsequently spectrally phase encoded, with the reception being performed by coherent homodyne detection using the synchronized receiver modelocked laser. The



key aspects of this approach are to use the optical frequency comb source in three different modalities that exploit the fundamental nature of phase coherent optical

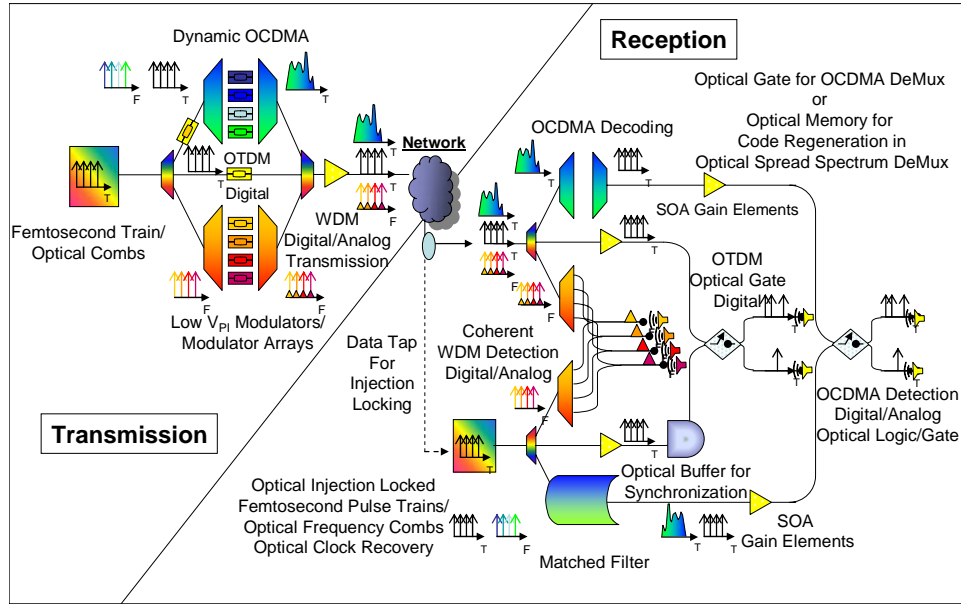


**Figure 1 Use of optical frequency combs for time domain, frequency domain, and code domain modulation formats**

frequency combs. These salient features are: 1) the short optical pulse duration generated (for OTDM formats), 2) the narrow linewidths and multiplicity of optical frequency components (for direct and coherent detection analog or digital WDM formats) and 3) the spectral phase coherence which will allow for frequency domain based coding techniques (for secure OCDMA formats) [3].

A second important application of modelocked lasers are in areas of microwave photonics, optical pulse shaping, optical sampling for analog to digital converters and for digital to analog converters for arbitrary waveform generation [4-9]. A unique feature of optical frequency combs is their ability to synthesize optical and RF waveforms. The generation of arbitrary optical and RF waveforms can be achieved by exploiting recent advances in the generation of stabilized optical pulse trains from modelocked semiconductor diode lasers [10-12]. In addition, the demonstration of arbitrary optical and RF waveform generation based on semiconductor optoelectronics provides a path for high performance imaging techniques based on a chip-scale semiconductor material platform that can be compact, efficient, cost effective and manufacturable. A simple illustration of a generic optical arbitrary waveform generator (OAWG) based on Fourier based frequency domain processing is shown in Figure 2. In this figure, the axial modes of a modelocked laser are frequency demultiplexed to allow the selection of a fixed number of independent axial modes,  $N$ . The amplitudes and phases of each mode can be adjusted to serve as the coefficients in a Fourier series basis, to generate an arbitrary waveform. Each mode is subsequently coherently combined using a spectral multiplexer

and the resultant optical waveform is generated. To detect the signal, a second set of stabilized optical frequency combs is spectrally demultiplexed and optically mixed with the synthesized signal, on a mode by mode basis. In this way, the modulation and detection bandwidths only need to be as wide as the axial mode spacing, and thus exploiting the truly parallel nature of this approach.

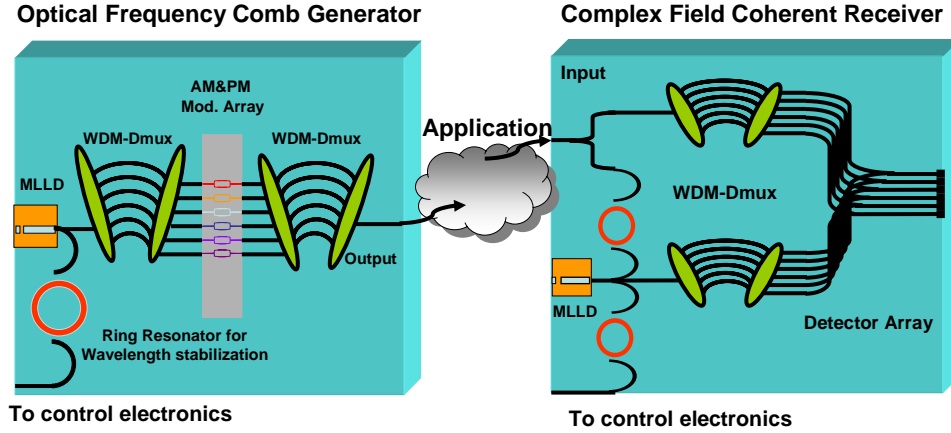


**Figure 2 Chip scale optical waveform generator and waveform detector based on optical spectral synthesis**

## Theory

The theoretical foundation of an optical arbitrary waveform generator is firmly rooted in frequency domain based Fourier synthesis techniques. The desired arbitrary waveform is generated by synthesizing a time varying intensity waveform by using a set of periodic, phase-locked (coherent) optical frequencies. The comb of optical frequencies is obtained by using a modelocked laser. The laser operates at a pulse repetition period of  $T$ , producing optical pulses with a pulse duration of  $t_p$ . The corresponding optical spectrum of the laser consists of a comb of periodically spaced, phase-locked optical frequencies, spaced at  $1/T$ , with the number of comb components approximately equal to  $N=T/t_p$ , (see Fig. 3). One can construct the desired waveform by considering the optical comb components as a discrete set of sinusoids that can be used to generate any periodic waveform by adjusting the relative amplitude and phase of each comb component. The generated waveform is given as [13]

$$f(t) = \frac{A_0}{2} + \sum_{k=1}^K A_k \cos(k\omega_0 t + \alpha_k) \quad (1)$$

where  $f(t)$  is the desired waveform,  $A_k$  are the Fourier coefficients for the amplitude,  $\alpha_k$  are the relative phase, and  $k$  is the comb component. In this case the generated waveform can be an arbitrarily designed waveform, constrained only by the number of comb components, and discrete values of amplitude and phase. The fidelity of the regenerated waveform owing to limited  $k$ , and discrete  $A_k$  &  $\alpha_k$ , can easily be quantified by using a least squares error analysis. Most importantly the reconstructed waveform is periodic at the period of the modelocked laser.

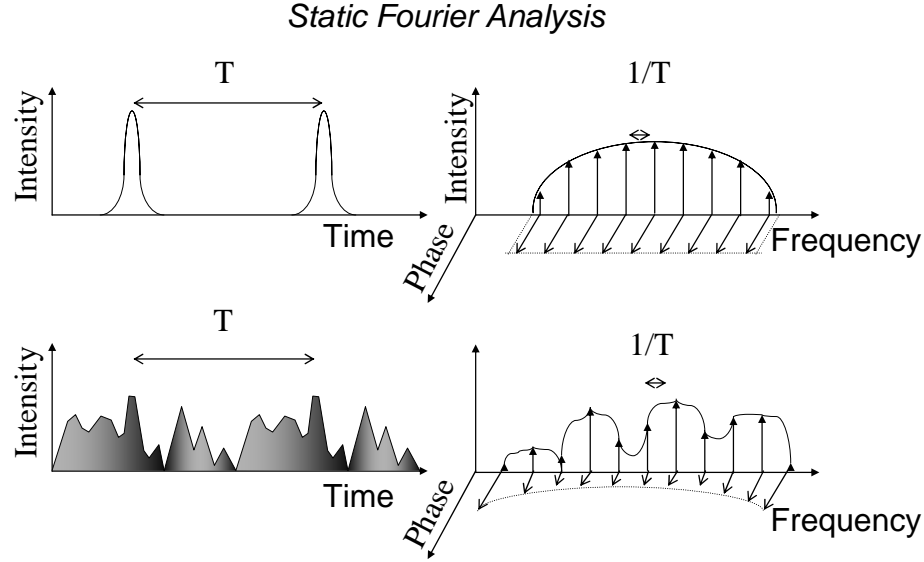


**Figure 3 Time and frequency representation of a modelocked optical pulse train and waveform generation by spectral filtering**

By extending these concepts to analog, time varying values of  $A_k$ ,  $\alpha_k$ , one can generate arbitrary waveforms that no longer appear periodic. This is depicted schematically in Fig. 4. The case of dynamic spectral modulation to create arbitrary waveforms can be modeled using a joint time-frequency representation of the desired waveform  $f(t)$  to be generated. For simplicity consider the “short-time Fourier transform”  $STFT(\omega, t)$ . In this formalization, information can be obtained about the ‘time-varying’ spectrum of a signal. Given that the amplitudes and phases of spectral components from the STFT can be specified, any arbitrary waveform can be reconstructed, assuming that the STFT exists. The short time Fourier transform is given by

$$STFT(\omega, t) = \frac{1}{\sqrt{2\pi}} \int f(\tau) g(\tau - t) \exp(-j\omega\tau) d\tau \quad (2)$$

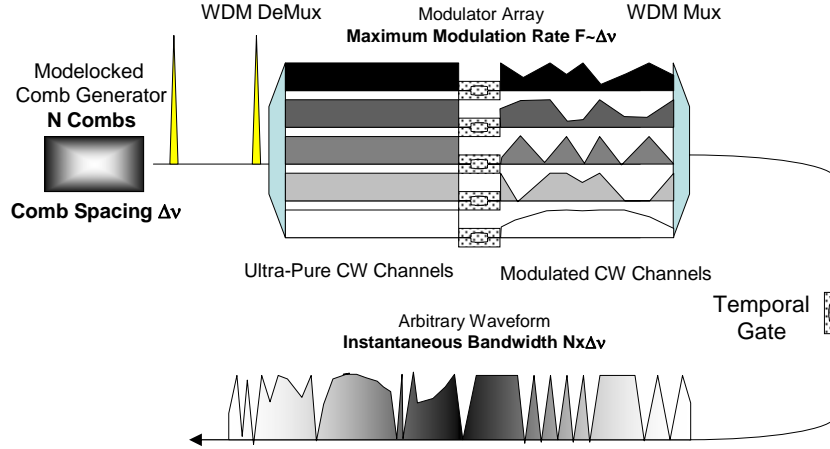


**Figure 4 Schematic of the process of waveform generation based on dynamic spectral modulation**

where  $f(t)$  is the reconstructed waveform and is given by

$$f(t) = \frac{1}{2\pi f^*(0)} \int \frac{M_{sp}(\theta, t)}{A_g(-\theta, t)} \exp(-j\theta t / 2) d\theta \quad (3)$$

In these equations,  $M(\theta, t)$  is the characteristic function or 2-dimensional Fourier transform of the magnitude squared of the STFT,  $A(\theta, \tau)$  is the ambiguity function, and  $g(t)$  is the gating function [14].

$$\begin{aligned} M_{sp}(\theta, \tau) &= \iiint |STFT(\omega, t)|^2 \exp(j\theta t + j\tau\omega) dt d\omega \\ &= A_f(\theta, \tau) A_g(-\theta, \tau) \end{aligned} \quad (4)$$

where

$$A_f(\theta, \tau) = \int f^*(t - \frac{1}{2}\tau) f(t + \frac{1}{2}\tau) \exp(j\theta t) dt \quad (5)$$

In this formulation, one can either know a priori how the amplitudes and phases are to be modulated and then construct the desired waveform, or conversely, design the desired signal and then generate the time varying amplitudes and phases that, when applied to the modulators, will generate the desired signal. It should be noted that the concept of frequency domain based pulse shaping is well founded, however, in those architectures, groupings of longitudinal modes are manipulated using liquid crystal modulators, which limits the waveform update rate to the kilohertz regime[4]. The current architecture provides for the highest possible spectral resolution which allows the pulse shapes to fill

the temporal window between pulses and also allows the waveforms to be updated at rates equal to the modelocked repetition rate. It should be noted that advances are being made in modulator array technology that will lead to improving the update rate in optical arbitrary waveform generators [15].

Some desirable output waveforms and capabilities of an OAWG would be to 1) generate ideal optical sine waves that should be continuously tunable over entire OAWG bandwidth, 2) generate ideal impulses where the pulse duration is limited in duration by the optical bandwidth of the OAWG, 3) generate every conceivable waveform within these limits, and 4) switch between waveforms as fast as possible. It should be noted that this approach is similar to other frequency domain based pulse shaping, with the salient difference being the spectral resolution used in each approach. In general, conventional pulse shaping architectures operates on grouping of longitudinal modes where as the approach illustrated here operates on individual longitudinal modes. This difference allows the OAWG to possess the highest possible resolution in waveform generation and fast update rates. In addition, the high spectral resolution provides the ability to completely fill the temporal window defined by the pulse repetition rate. Finally, the OAWG possesses the capability to generate pure arbitrary cw signals as well as arbitrary pulsed signals.

## **Simulation of Test Waveforms**

### *Time Domain Interleaving for Arbitrary Sinewaves and Chirps*

This section shows simulations of some selected waveforms. The purpose of the simulations are to show the specific challenges that may limit the performance associated with frequency domain based OAWGs and highlight potential solutions for these limitations. The simulations are performed in Matlab. A set of complex optical carrier frequencies is used. The optical comb components are equally spaced in frequency, with time varying amplitudes and phases. The optical frequencies are coherently added to generate the desired signal. To illustrate some key challenges, the intensity of the desired signal is calculated, since the receiver scheme for OAWGs rely on coherent optical hetero- or homodyning, where the mixed optical intensity is photodetected.

To illustrate a key challenge, consider the generation of a single arbitrary sine wave. It is well known that by using the comb of a modelocked laser, well defined sinewaves can be generated, but only at discrete frequencies. On the other hand, the concept of serrodyning can be employed to convert any one of the discrete frequencies from an optical frequency comb to an arbitrary frequency [16-18]. This is most easily achieved by imparting a linear phase ramp to one of the comb components (see Figure 5). In this case, a time varying linear phase ramp impressed on a sine wave results in a static frequency shift of the original sine wave. The challenge of this serrodyning approach to generate an arbitrary frequency results from the practical nature of common optical phase modulators, in that these modulators are can not be driven with continuously increasing voltage to increase the phase. Generally, when the applied voltage reaches a value on the

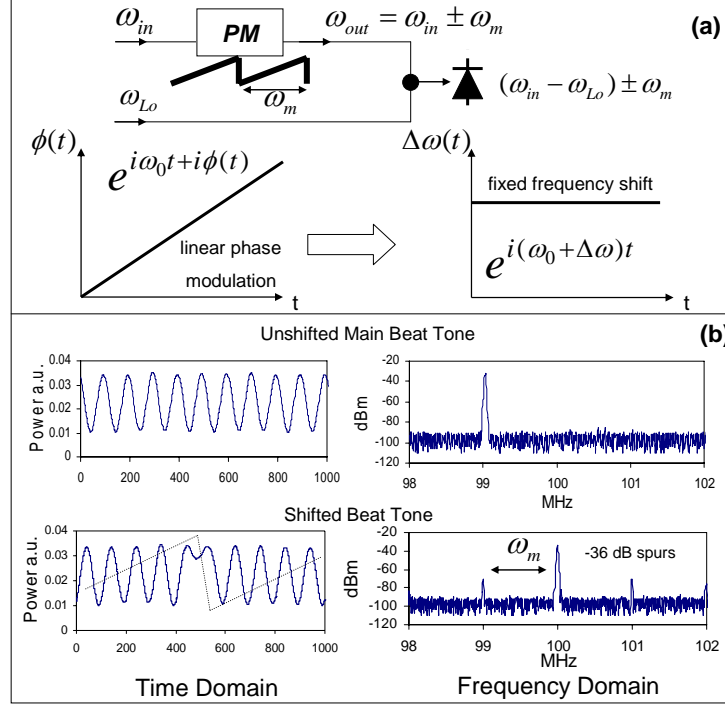


**Figure 5 Concept of serrodyne modulation. (a) Experimental configuration and mathematical representation, (b) Experimental results showing the original tone and the shifted tone with spurs due to the finite fall time of the phase modulator**

order of  $V_\pi$ , the applied voltage needs to be ‘reset’ such that the phase modulation can continue. During this ‘reset’ time, since the fall time of the modulator is not infinitely fast, the linearity of the phase modulation is interrupted, thus creating unwanted frequency components in the generated signal. Figure 5 shows a simple schematic for creating a serrodyne waveform, along with time and frequency domain plots of the waveform and power spectra, respectively. Note that when the phase modulation is being reset, the temporal waveform is corrupted which results in additional frequency components, or spurs, in the power spectrum. One possible solution to this problem is to use a time domain based interleaving approach to assist in suppressing the unwanted frequency components associated with the finite bandwidth of the phase modulators [19]. This approach is conceptually illustrated in Figure 6, and described below.

The modelocked comb is split into two identical combs. Waveform generation is performed on one comb set, while the second comb set is off (intensity modulators in the off state). As the applied voltages on the phase modulators approach the maximum allowed value, the intensity modulators turn off these combs and the phases are allowed to reset. As the combs from set one are being turned off, the intensity modulators of comb set two are turned on, with the appropriate phase modulation, to continue the waveform generation process. Thus, the OAWG generates two waveforms that are temporally interleaved to create a single continuous waveform. In this case, the detrimental effect of finite fall time of the phase modulators is suppressed since the

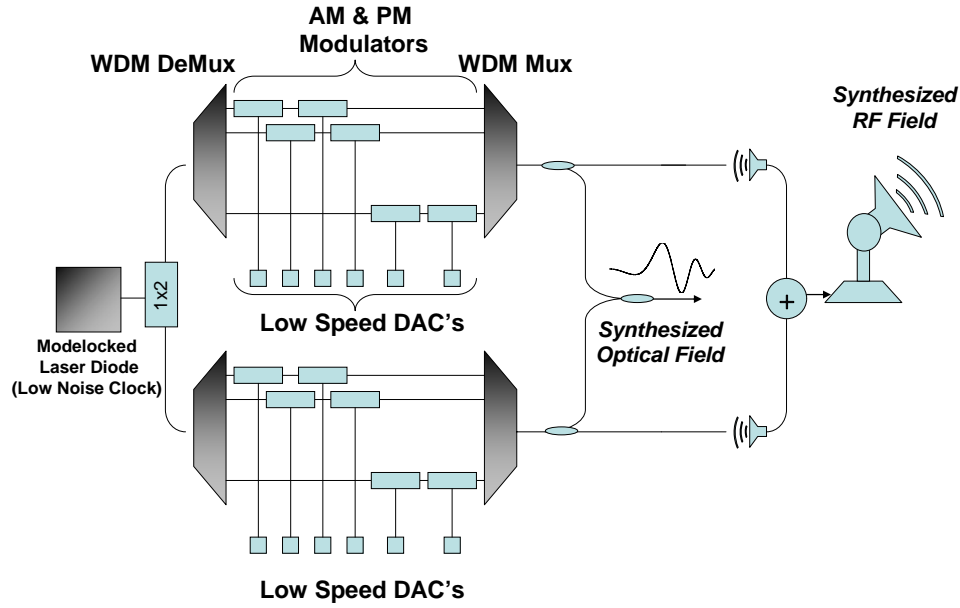


**Figure 6 Use of two frequency comb sets in a time domain interleaving configuration for the suppression of spurs**

phases are being reset while the combs are off. This results in a generated arbitrary waveform without the creation of unwanted frequency components. In this geometry, the maximum modulation bandwidth required for the modulators is equal to the longitudinal mode spacing, or repetition rate of the modelocked laser, which physically allows the longitudinal modes to fill the bandwidth between modes. It should be noted that there may be different modulation algorithms to generate a particular arbitrary waveform. The particular modulation algorithms to generate each waveform were chosen to allow for analog waveforms applied to the phase modulators and digital waveforms applied to the amplitude modulators. This was done to exploit the excellent linearity inherent in many phase modulators, and reduce the linearity requirement for amplitude modulators. It should be noted that in addition to the generation of arbitrary optical waveforms, arbitrary RF waveforms can also be generated by optically detecting the individual signals from both AWG's and electrically combining the photocurrents. In this case, one has the ability to perform both coherent and incoherent addition of the optical fields.

To further illustrate the operation of the OAWG using time domain interleaving for spur suppression and some inherent challenges, simulations of several waveforms were generated. These waveforms were: 1) an arbitrary single tone, 2) two arbitrary tones, 3) a linear RF chirp and 4) a unit step tone.

### Arbitrary Single Tone via Serrodyning

An arbitrary single RF tone can be achieved by combining two optical frequency components, with a frequency separation  $\Delta f$  near the desired frequency,  $\Delta f + \delta f$ . The desired RF waveform is obtained by impressing linear phase modulation onto one of the carriers and combining the result onto a photodetector. The derivative of the time varying voltage applied to the phase modulator determines the addition frequency shift  $\delta f$ . Thus, in general, the frequency shift obtained is inversely equal to the time it takes for the phase modulator to vary from 0 to  $V_\pi$ . Fig. 7 shows the timing diagram for the applied voltages, as applied to both coherent comb sets, to realize the desired intensity and phase modulation to achieve an arbitrary single tone with serrodyning, as required by the time domain interleaving concept to avoid spurs generated from the finite reset time of the phase modulators. Note that as the phase is returning to zero volts in AWG 1, the intensity of that comb component is zero, and the waveform generation process is governed by AWG 2. Figure 8(a-c) shows the temporal output from the individual

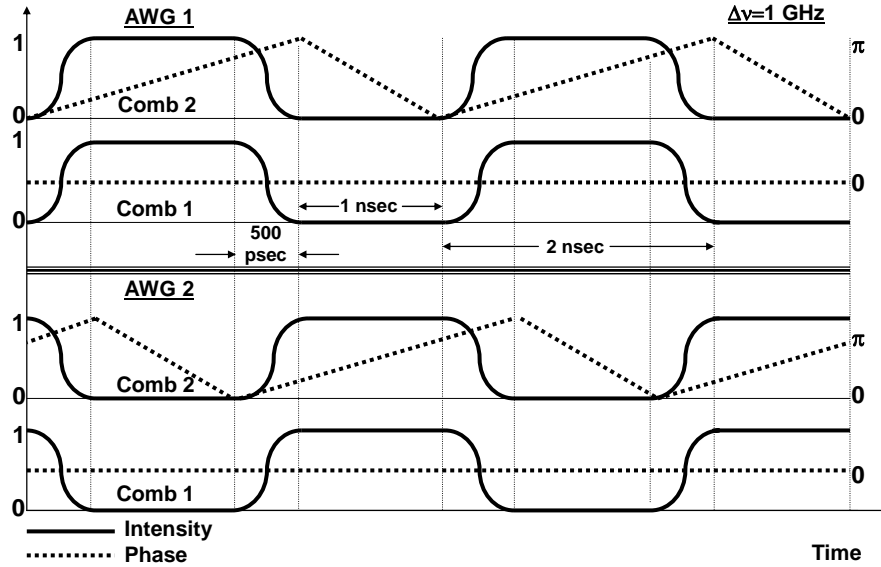


**Figure 7** Timing diagram of the applied signals to individual comb components to generate a single arbitrary tone, using time domain interleaving for spur suppression



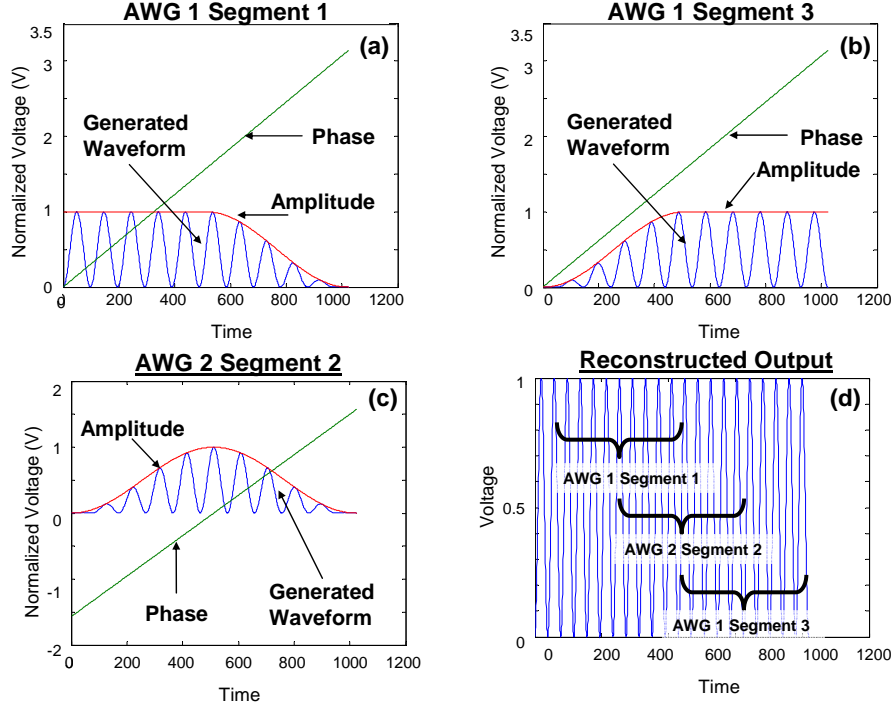


**Figure 8 Simulated plots of the generated waveform for the arbitrary single tone timing diagram in Figure 7**

waveform generators, highlighting the intensity and phase variations, while Fig. 8(d) shows how each of the three temporal segments represented by Fig. 8(a-c) are temporally interleaved to generate a continuous arbitrary RF tone.

### *Two Arbitrary Tones*

The arbitrary two tone waveform is not directly obtained from an extension of the single tone case. Nonetheless, by using three optical carriers, one can obtain any two desired arbitrary RF waveforms and a cross-product RF tone at the sum frequency of the two tones. By low pass filtering, the desired arbitrary two tone signal is obtained. Figure 9 shows the timing diagram to produce a continuous arbitrary two tone signal.

The key penalty for this algorithm in generating a two tone signal is that one requires twice the optical bandwidth for a desired RF bandwidth. In Figure 10(a) shows the generated time domain signal obtained by combining three optical carriers, with one center carrier and two optical carriers at higher and lower offset. By phase modulation of the Stokes and anti Stokes carriers, the two tones are generated. An additional RF component is generated at the sum frequency and is shown in the power spectrum (Fig. 10(b)).

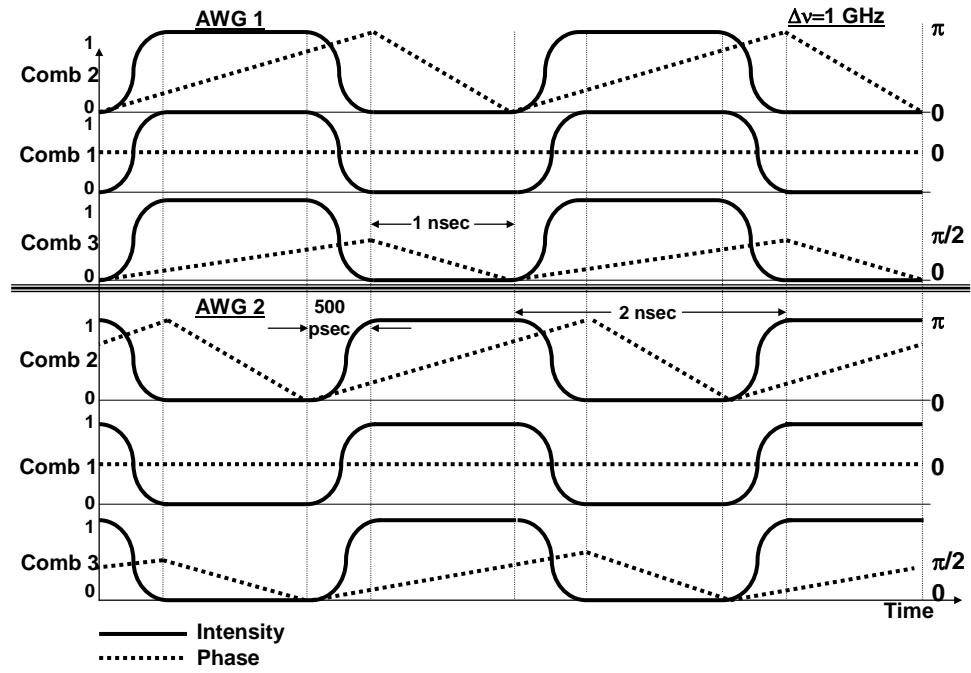


Figure 9 Timing diagram of the applied signals to individual comb components to generate an arbitrary tone signal

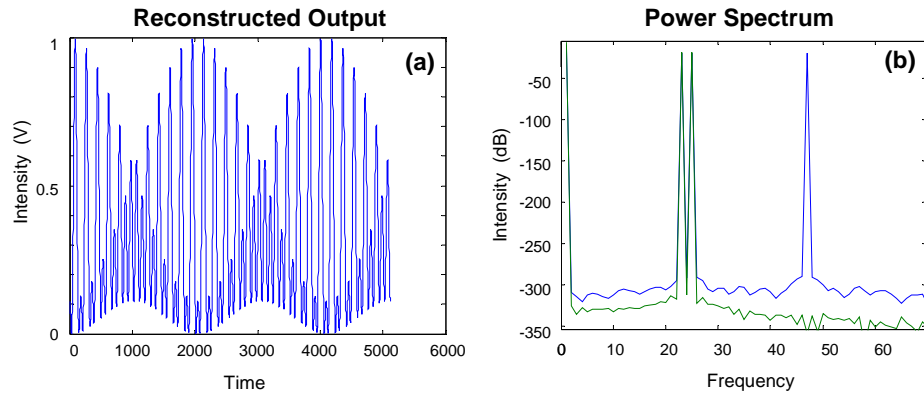


Figure 10 Simulated plots of the generated waveform for the arbitrary two tone timing diagram in Figure 9

### *Linear RF Chirp*

An arbitrary, intensity modulated linear chirp can be constructed by switching between multiple frequency comb bins of the OAWG. As an example, the desired linear chirp can be generated as follows: The starting frequency is chosen to be the frequency difference from two carriers. Quadratic phase modulation is applied to carrier 1, which chirps the signal to a frequency equal to the difference between carrier 1 & 3. Quadratic phase modulation is repeated on carrier one as carrier 2 is turned off and carrier 3 is turned on. The process is repeated until the desired stop frequency is obtained. The timing diagram for the intensity and phase modulators using the time domain interleaving concept is shown in Figure 11. The simulated time domain output waveforms for the different interleaved temporal components of the composite waveform and the corresponding power spectrum of the composite waveform is shown in Fig. 12.

### *Single Tone Unit Step Function*

An alternate algorithm to generate waveforms utilizes a combination of time domain interleaving and pulse shaping. Consider for example, the generation of a transient waveform, such as the single tone unit step function. In this case, the intent is to instantaneously turn on a single tone. The challenge arises owing to the limited bandwidth of the modulators and the large bandwidth required that exists during the rising edge of the generated waveform. This can be achieved by slowly turning on a single tone with AWG 1 and designing a pulse shape from AWG 2 that represents that

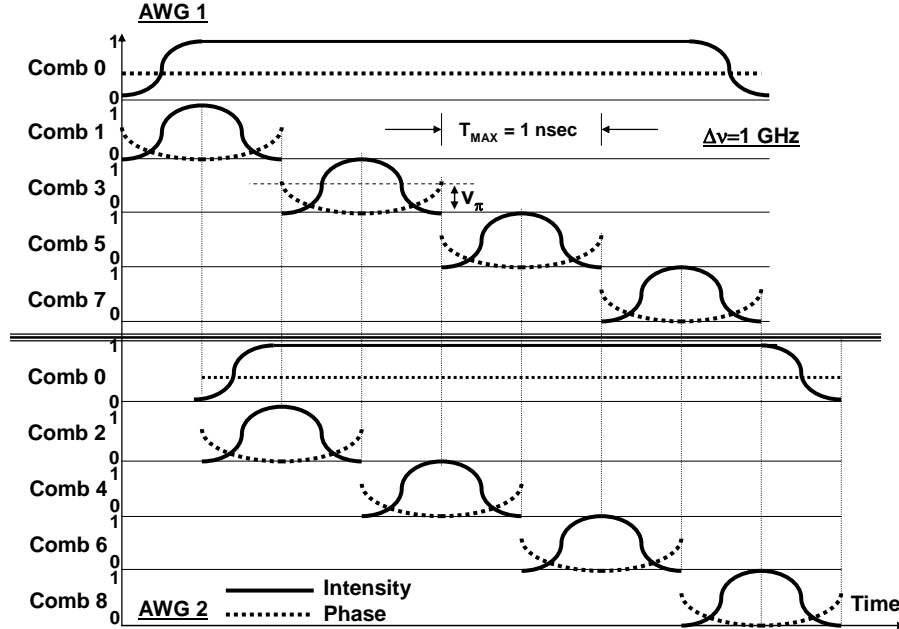


**Figure 11** Timing diagram of the applied signals to individual comb components to generate a chirped signal

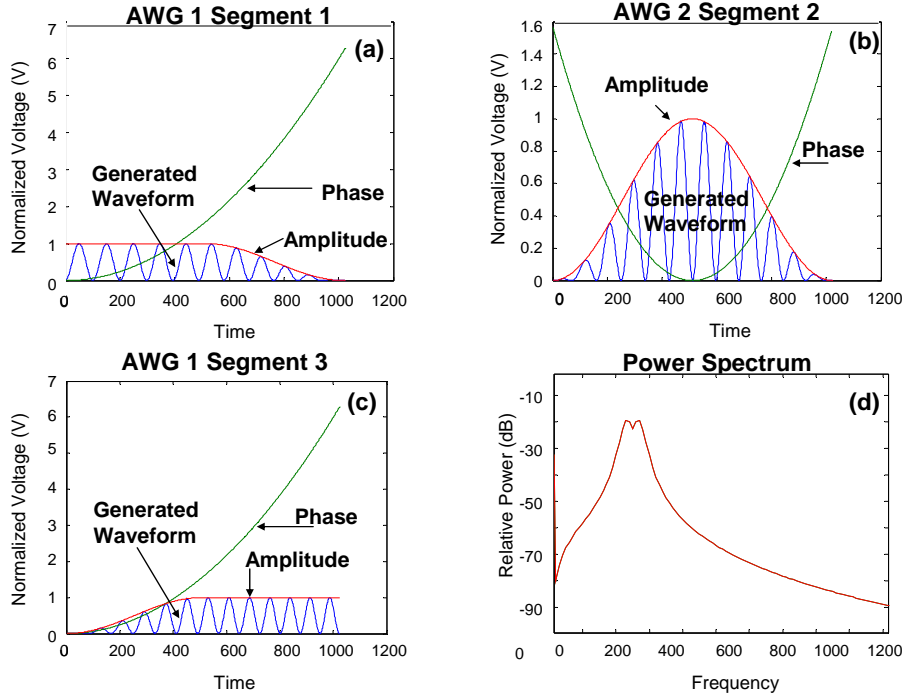


**Figure 12 Simulated plots of the generated waveform for the chirp timing diagram in Figure 11**

portion of the generated waveform that is not desired in the final output. By differentially combining the detected photocurrents, an approximation of the desired waveform is generated.

The limitation of this approach is that the generated waveform is an approximation to the desired waveform since the shaped pulse is only an approximation of the undesired part of the waveform generated by AWG1. The approximation is due to the finite number of combs used to generate the shaped pulse. By using more frequency combs, a better approximation of the shaped pulse is obtained, leading to a better approximation to the desired waveform. In Figure 13 are the waveforms generated from AWG1 (Fig. 13(a)) and an approximation of the shaped pulse from AWG2 (Fig. 13(b)). The differentially combined photocurrent is shown of the desired waveform (Fig. 13(c)), along with the RF power spectrum of the generated waveform (Fig. 13(d)). For comparison, in the RF power spectrum, the power spectrum of a periodic square wave tone is plotted, which highlights the similarities and differences. Most notable is the broad spectral feature in the power spectrum of the generated waveform which results from the finite number of combs used to generate the pulse shape creating the rising edge of the desired waveform.

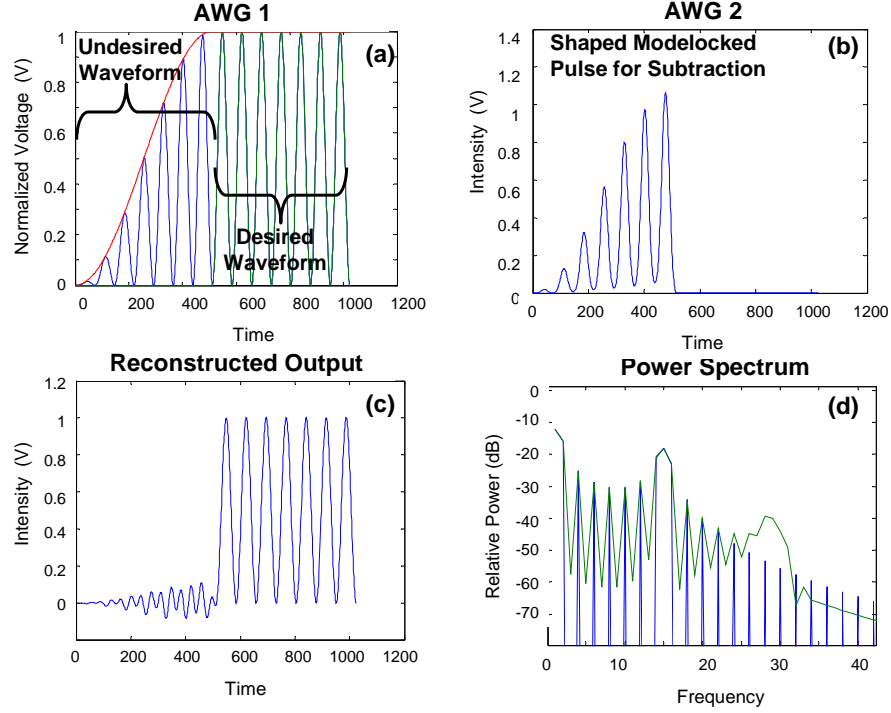


**Figure 13** Simulated plots of a generated waveform using both pulse shaping and dynamic modulation schemes to generate a ‘step-like’ transition on a carrier frequency

## **Experiments**

### *Comb Technology*

To realize a functional arbitrary waveform generator based on dynamic Fourier synthesis of an optical frequency comb, the quality of the optical comb source will determine the ultimate performance of the AWG. In addition, since the optical combs must be demultiplexed for AM and PM modulation and subsequently re-multiplexed, the optical frequency comb must be stabilized so there is no drift of the frequency comb with respect to the comb demultiplexer. To achieve this, the modelocked laser must be frequency stabilized. Currently, the approach being explored for the generation of stabilized optical frequency combs is to construct an external cavity harmonically modelocked semiconductor laser in a ring configuration and incorporate an intracavity, high finesse etalon that will serve to select the operation of a single longitudinal mode grouping [20]. This technique was shown to be instrumental in developing ultra low timing jitter optical pulses and is called “supermode suppression” [21]. In addition, a feedback loop to control and stabilize the laser is used [22]. The stabilization method is the standard “Pound-Drever-Hall” (PDH) technique [23]. Figure 14 shows a schematic diagram of the external cavity modelocked laser that employs an intracavity etalon to allow for the suppression of unwanted optical frequencies (supermode suppression) to generate a set of stabilized coherent optical frequencies. Additional stabilization and noise reduction is realized using a second phase locked loop that minimizes the long term, low frequency noise.

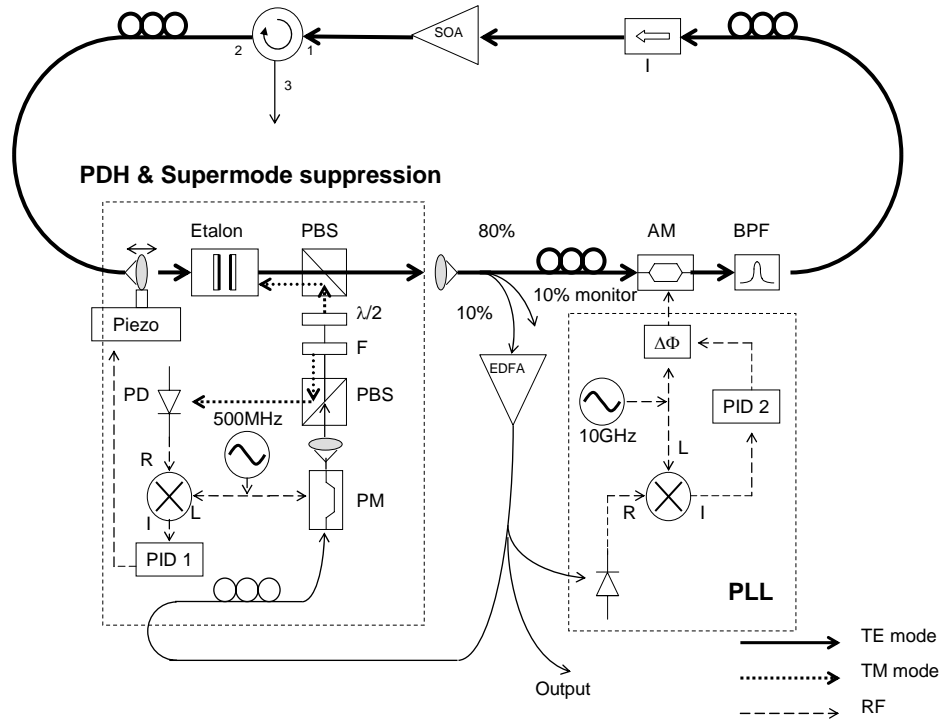


**Figure 14 Schematic of a harmonically modelocked ring laser using an intracavity etalon to select a single longitudinal mode group and suppress supermode noise competition**

The current performance of the optical comb output is shown in Figure 15. This figure highlights the output characteristics of the comb generator, which shows the optical frequency comb, the intensity autocorrelation, a heterodyne beat measurement that provides information on the long term frequency stability and linewidth of an individual comb component, and the residual phase noise (Fig. 15(d), left axis), or timing jitter (Fig. 15(d), right axis), of the modelocked comb, measured to offset an offset frequency equal to half the pulse repetition rate [24, 25]. The average output power of the laser oscillator is 0.02 mW and subsequently amplified to 20 mW using an erbium doped fiber amplifier. The output pulses are ~17 psec and are ~4 times the transform limit, with a predominate linear chirp impressed on the pulses owing to the modelocking dynamics.

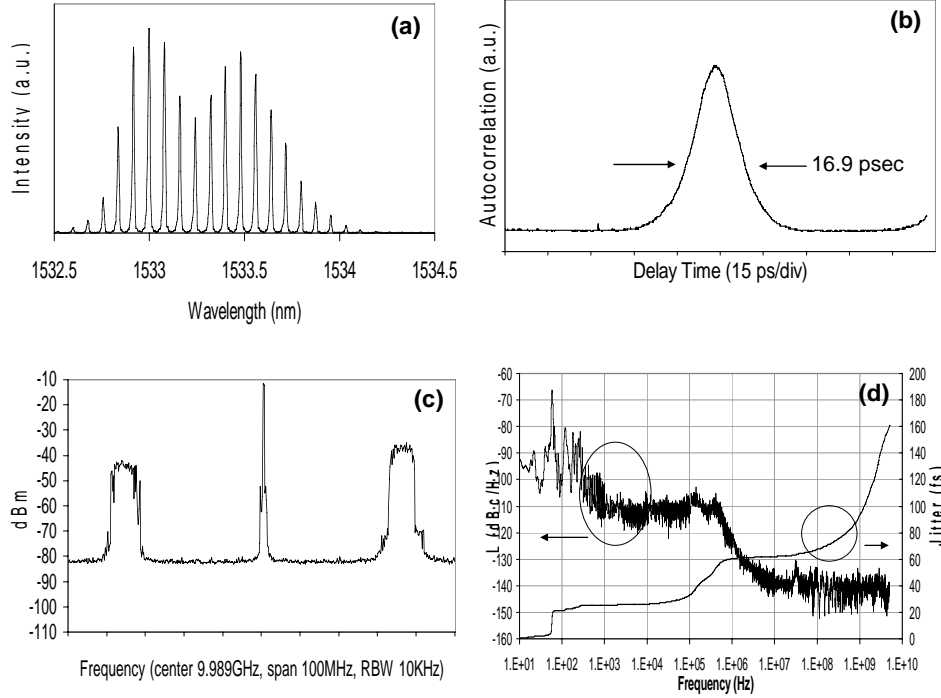


**Figure 15** Output characteristics of the frequency stabilized harmonically modelocked laser. (a) Optical frequency comb, (b) intensity autocorrelation, (c) heterodyne beat measurement showing the frequency drift of the stabilized comb, and (d) the residual phase noise plot, along with the integrated timing jitter values

#### Optical Comb Frequency Channelizing Filter Technology

In order to obtain access to the individual components of the optical frequency comb, the spectrum must be demultiplexed. This can be achieved by a variety of optical frequency filter technology, the choice of the filtering technology being dependent on the periodicity of the frequency comb. For modelocked lasers with repetition rates on the order of several gigahertz, the frequency demultiplexing technology can rely on etalon based demultiplexers, such as the virtually imaged phased array (VIPA) filters or ring resonator based technologies [26-29]. Key aspects of the filter technology are the flatness of the filter channel, the crosstalk between filter channels, the steepness of the filter edges, and dispersion within individual filter channels and dispersion across the full filter bandwidth. In addition, the filtering technology must be frequency matched, with respect to separating the channels and remultiplexing them subsequent to modulation. As an example, Figure 16 shows overlaid plots of the experimentally measured frequency spectra of the individual channels from an etalon based frequency demultiplexer that have been used for experimental results described below. For this filter, the channel to channel spacing was designed for 6.25 GHz, with 16 output channels. Owing to the etalon nature of the demultiplexer, the filter has a free spectral range of 100 GHz, implying that output combs separated by 100 GHz will be present on a single output channel. The overall

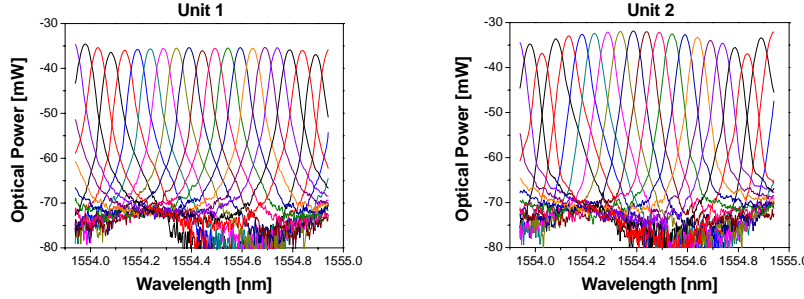


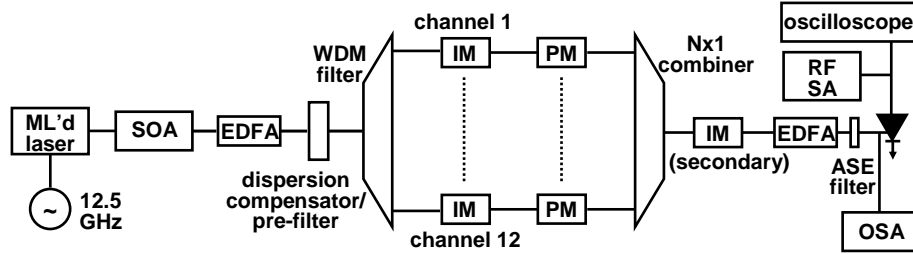
**Figure 16** Overlaid spectral plots of the individual channels of the frequency demultiplexer pair

insertion loss is  $\sim -7$  dB, with a channel to channel crosstalk between filter channels of  $\sim -15$  dB. For some of the experiments carried out, a pulse repetition frequency of 12.5 GHz was used to improve the channel to channel cross talk. It should be noted that depending on the filter technology, the dispersion characteristics may vary independently across each channel, which would lead to impairments in the fidelity in waveform generation. By characterizing the dispersive property across each channel, the overall impairments can be reduced by predistortion techniques applied to the phase modulators.

#### Waveform Generation Results

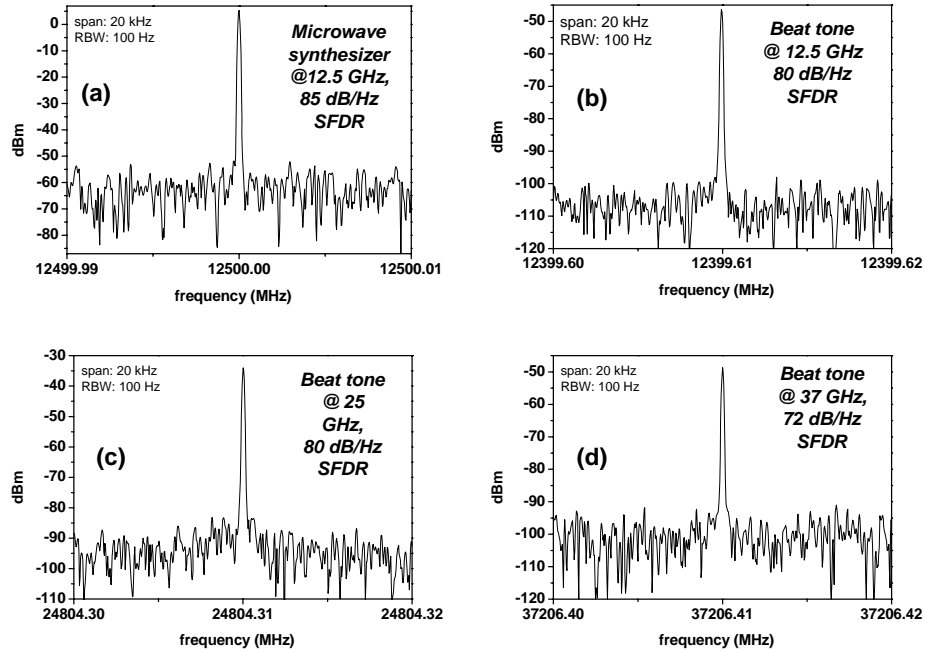
A prototype arbitrary waveform generator was realized by using a fundamentally modelocked external cavity modelocked diode laser operating at a pulse repetition frequency of 12.5 GHz. This was chosen to be twice the channel to channel spacing of the frequency demultiplexer described above, in order to improve the channel to channel crosstalk performance. A schematic of the setup is shown in Figure 17. Only one AWG is experimentally used, since the generated waveforms shown in this section do not require temporal interleaving. The optical combs were amplified in an SOA/EDFA amplifier chain, and subsequently passed through a dual grating dispersion compensator with an adjustable slit in the Fourier plane, to limit the input bandwidth to 100 GHz, and to suppress unwanted background spontaneous emission. The laser produces optical pulses of  $\sim 1$  psec after dispersion compensation and contained over 40 comb components within the -3dB bandwidth prior to filtering. Owing to the fundamentally modelocked nature of the comb source at 6.25 GHz, and the finite finesse of the laser cavity, the individual comb components possessed a linewidth of  $\sim 50$  MHz.





**Figure 17** Experimental configuration of the arbitrary waveform generator

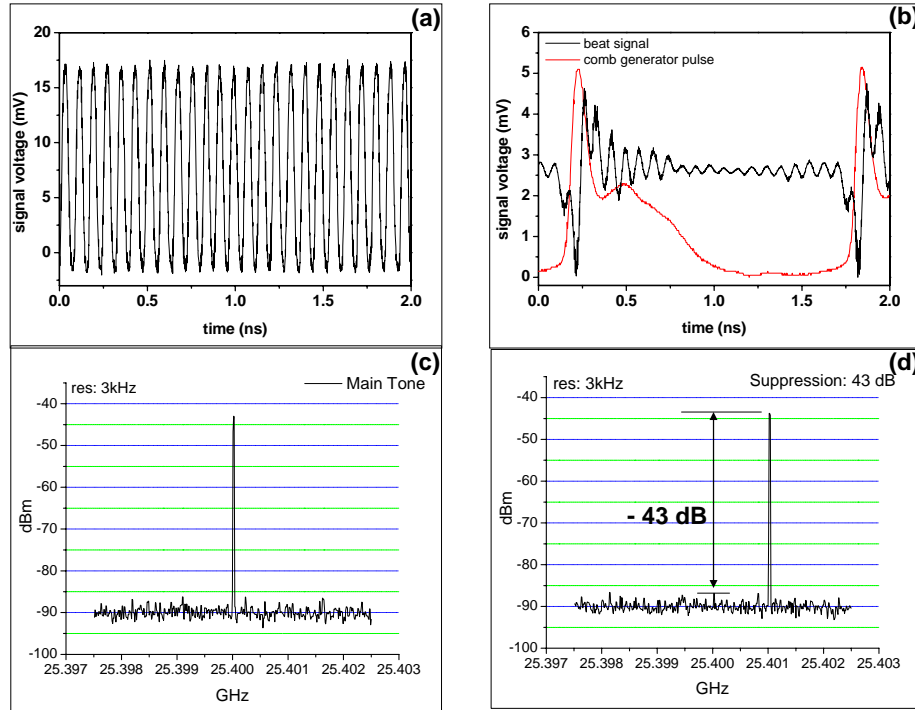
To test the potential performance of the AWG, beat note measurements between several independent comb components were performed to determine the optical comb fidelity, the linewidth of the RF beat note, and the optical comb to comb frequency drift. The results of these measurements are summarized in Figure 18.



**Figure 18** RF beat notes generated by selected individual optical comb components

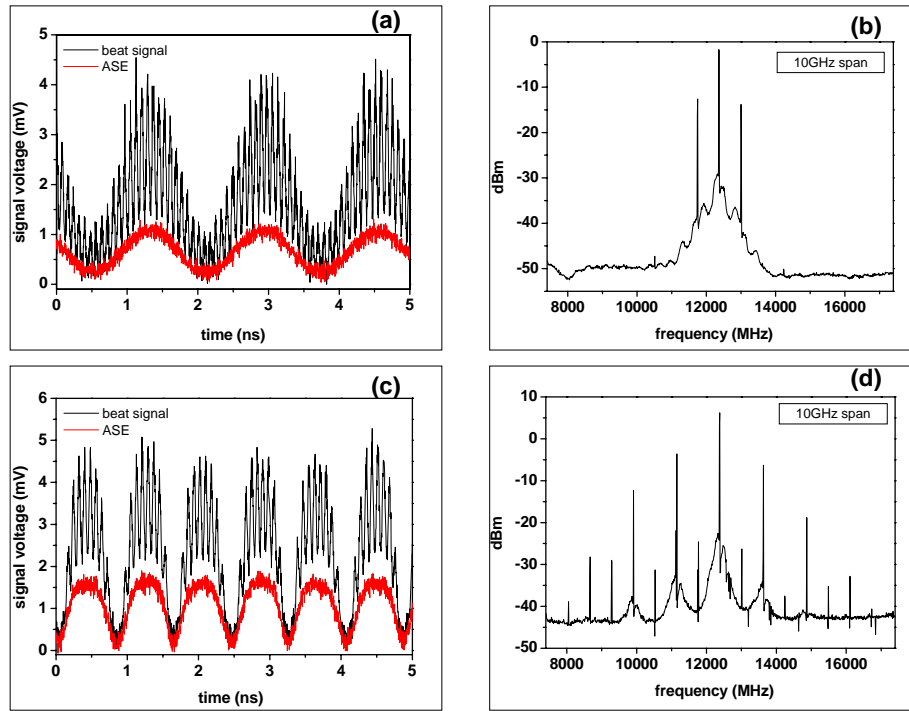
The salient features in this data set are the measured high dynamic range of the beat notes ( $\sim 85$  dB/Hz) as compared to the microwave synthesizer used to modelock the laser, and the narrow linewidth of the beat note which was resolution limited using a 100 Hz filter. The former shows that high quality, synthesizer like beat notes can be achieved, and the latter shows that despite the 50 MHz optical linewidth of a comb component, the beat notes are all resolution limited, below 100 Hz. This shows that the optical phase noise is correlated across the spectrum, and that the relative comb to comb drift is less than 100 Hz.

To demonstrate the agility of the AWG, modulated sine waves, RF bursts, RF chirps, and arbitrary frequency sinewaves were generated using the time domain interleaving serrodyne approach. Figure 19(a) show temporal outputs of a sine wave produced by two comb components, while Fig. 19(b) shows the temporal output of the same beat signal being modified to generate an RF burst. Figure 19 (c) shows an RF spectrum of a two comb beat signal at 25.4 GHz and an RF spectrum of an arbitrarily shifted tone generated by the time domain interleaved serrodyne approach [30]. In the case of the serrodyne time domain interleaved case, the resultant RF tone is able to suppress the undesired spurs down to a level of -43 dB below the carrier. This level of spur suppression is currently limited to the extinction ratio ( $\sim -20$  dB) of the intensity modulators using in generating the waveform. Current state of the art intensity modulators have been shown to possess extinction ratios on the order of 60 dB, which could lead to spur suppression on the order of -120 dB.



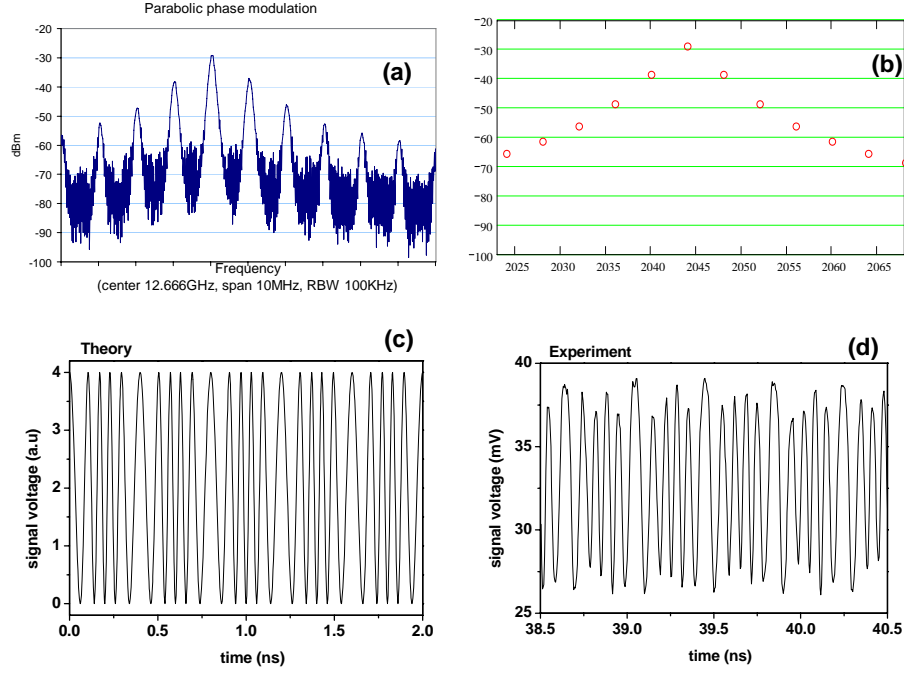
**Figure 19** Experimental results of dynamic modulation, showing the generation of RF bursts, and arbitrary RF tones, using serrodyning and time domain interleaving

Figure 20(a-d) show additional temporal and spectral plots of the arbitrary waveform generator using dynamic modulation. In these data, a 12.5 GHz RF tone generated by combining two comb components is further modulated using a conventional LiNbO<sub>3</sub> modulator. The comb components were amplified with an erbium doped fiber amplifier (EDFA), in order to measure the RF spectrum with high dynamic range. For these plots, the LiNbO<sub>3</sub> modulator was dc biased at quadrature (Fig. 20(a,b), and at the minimum transmission point (Fig. 20(c,d)). The resultant modulated signal is seen to ride on top of a modulated dc background which is due to the background spontaneous emission created by the EDFA. As a result, the measured RF spectra show the spectral peaks expected from Fourier analysis, however with added noise bands as exhibited by the broad pedestals accompanying the discrete spectral components.



**Figure 20 Modulated sine waves and their corresponding RF spectra**

Figure 21(a-d) shows an example of chirp generation. For this waveform, a two comb beat signal at 12.5 GHz was generated and subsequently phase modulated using a sinusoidal signal. Typical experimentally generated outputs are shown in Fig 21(a,d) highlight the spectral and temporal characteristics, while data for a simulation of this case are shown in Fig. 21(b,c). Note the good agreement between the experimentally measured outputs and their corresponding simulations.



**Figure 21** Experimentally measured RF chirp spectrum (a) and its time domain counterpart. (b,c) simulations of the spectral and temporal output respectively

### Coherent Detection Communications and Signal Processing

This section briefly introduces and describes one approach of using the optical frequency combs for either detecting an arbitrarily synthesized electric field (recall Fig. 2) or for coherent communications using a set of re-generated optical combs at the receiver to serve as a set of optical frequencies for a local oscillator receiver array. Recall in Figure 1 shows an illustration of using the optical frequency comb generated from a master oscillator modelocked laser (MO-MLL) as a set of discrete carriers of information. Key to this approach is the use of a second set of optical frequency combs from a local oscillator modelocked laser (LO MLL) that will serve as coherent probes in a parallel, dense WDM coherent receiver arrayed architecture. The second set of optical frequency combs can be made optically phase coherent by optically injecting a portion of the MO-MLL light into the LO MLL. The optical injection establishes coincidence in the optical frequency, phase and comb spacing between the two sources. The resulting phase locked optical frequency combs can now be used in a variety of coherent homo- or heterodyne detection schemes [31-33]. Figure 22 illustrates a configuration for a coherent receiver in an optical code division multiplexed communication system. The desired coded signal is properly decoded by using a set of optical frequency combs phase locked to the transmitter. The receiver local oscillator combs have either the identical code, or the code conjugate. The received signal is coherently detected, on a comb by comb basis, with the resultant beat signal of each channel summed coherently in the electrical domain to reconstruct and detect the received signal, completely suppressing the multi-user interference.

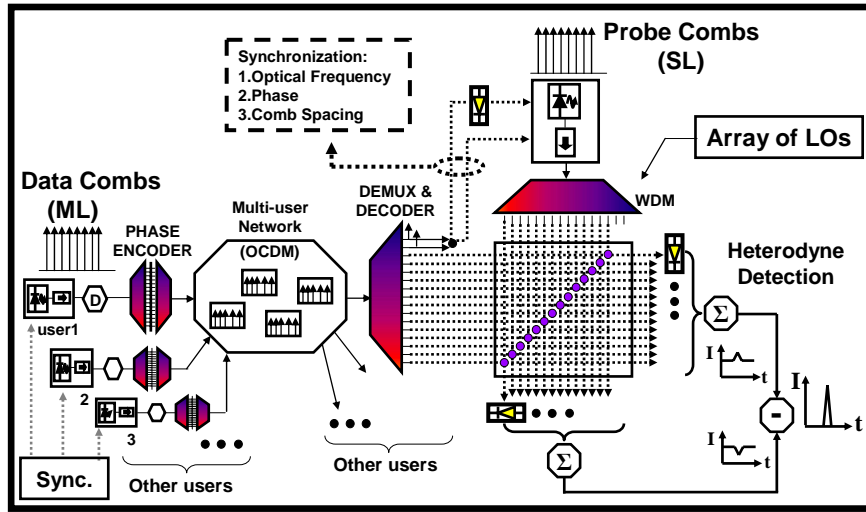


Figure 22 Schematic illustration of the use of optical frequency combs and injection locking to realize a coherent OCDMA receiver

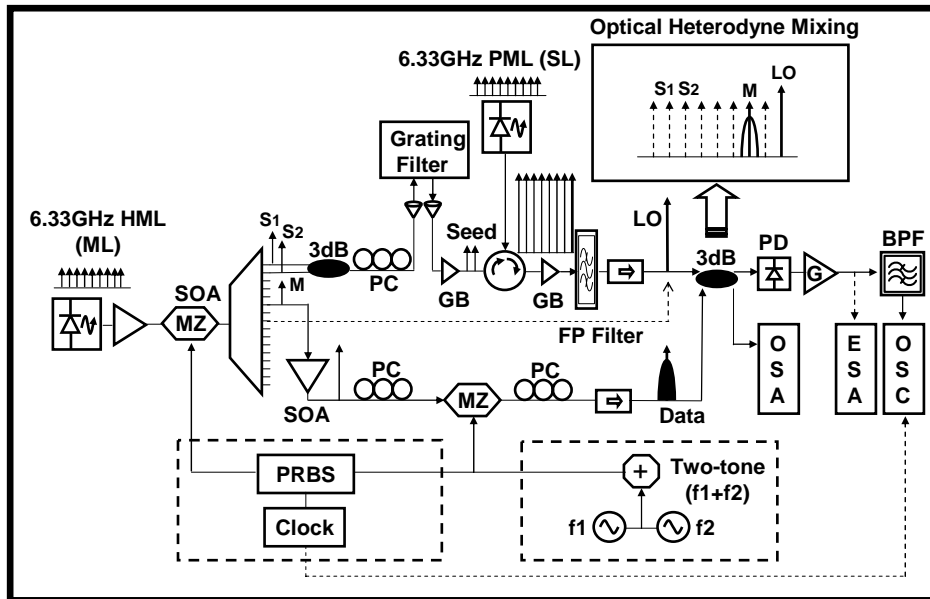
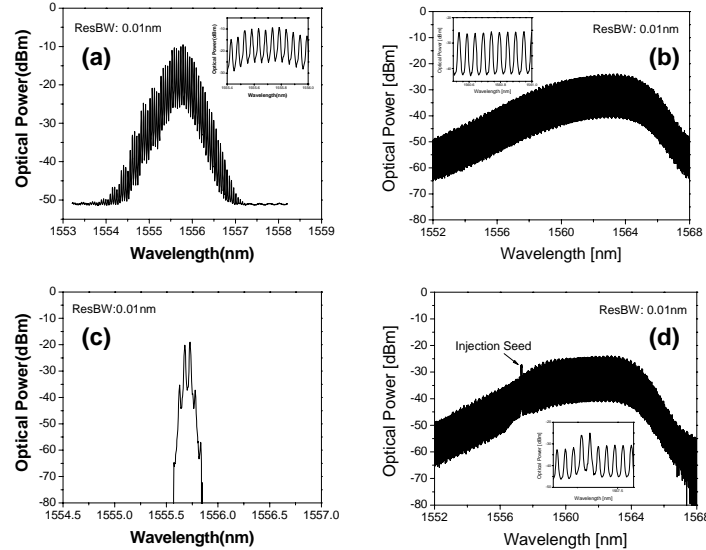


Figure 23 Experimental setup demonstrating the use of optical frequency combs, injection locking and coherent detection for both analog and digital modulation formats

To support this concept, a key element is associated with recovering a set of optical frequency combs phase locked to the transmitter. This can be achieved by optically injecting at least two comb components from the transmitter into a passively modelocked laser [34-36]. The salient feature for the requirement of at least two optical comb components for recovering a set of phase locked combs is that, in addition to the fact that the optical injection establishes the frequency and phase of the slave laser, at least two comb components are required to define the pulse repetition rate [37]. In Figure 23, an experimental configuration for using optical frequency combs for coherent analog and digital communications is illustrated, where the receiver local oscillator combs are made to be frequency and phase coherent with the transmitter laser by optical injection locking using two axial components of the transmitter laser. In this experiment, the modelocked laser operates at 6.33 GHz, to match the demultiplexer used in this experiment. Two axial modes from the master laser,  $S_1$  and  $S_2$ , are used as optical seeds to injection lock the slave laser. A single axial mode,  $M$ , is the channel that will carry either analog or digitally modulated information. The selected tone from the slave laser, LO, is used as the local oscillator for coherent detection. It should be noted that the seed tones, the modulated carrier and the local oscillator are separate and distinct optical frequencies, to assure that the coherent performance is properly measured, without any added benefit of these signals being frequency coincident with each other.

Spectra of the master laser, the slave laser under passive modelocked conditions, the selected two tones used for optical injection, and the slave laser under injection locked conditions are summarized in Figure 24. It should be noted that the external cavity of the



**Figure 24** (a) Output spectra of the hybrid modelocked transmitter laser (master), (b) output spectra of the passive modelocked laser (slave), (c) selected two tones from the master laser, (d) injection locked slave laser

the master laser was configured with a diffractive grating as a feedback element to limit the modelocked spectrum, which allowed the master laser to generate higher optical power per mode and facilitate the optical injection locking process. Performance of optical injection locking of the slave laser is summarized in Figure 25. Both the injection locking power requirements and injection locking bandwidth were measured. An output characteristic of the slave laser that exhibited a large reduction in the noise sidebands of the RF power spectra under injection locking conditions was indicative of the slave laser being locked. From these measurements it was found that robust locking of the slave laser could be achieved with  $\sim -30$  dB of injection power. To determine the locking bandwidth, the master laser was detuned from the slave laser by adjusting the applied RF frequency. With  $\sim -20$  dB of injection power, a locking bandwidth of 3 MHz was achieved. These results clearly demonstrate the robustness of optical injection locking for synchronizing independent modelocked laser sources.

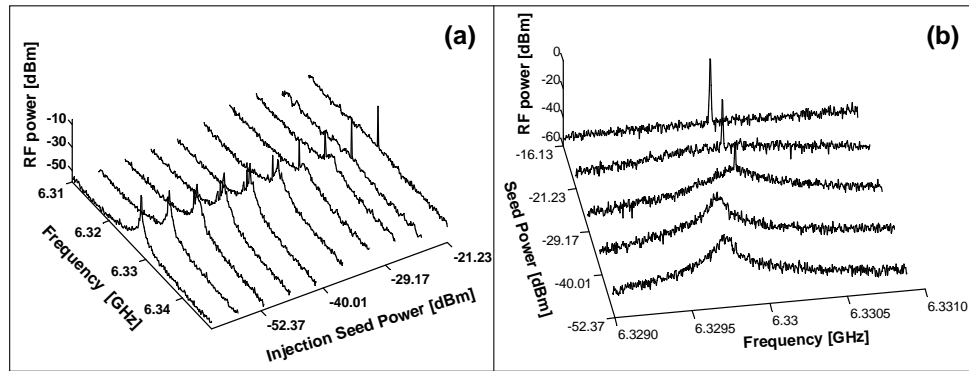


**Figure 25** Locking dynamics of the injection locked passive modelocked laser. (a) Series of spectra for increasing injection power, (b) series of spectra showing the locking range (fixed detuning and increasing injection power)

To further determine the robustness of the injection locking process, the recovered optical frequency combs were demultiplexed and used as coherent local oscillator tones to detect both a two-tone analog signal and a pseudo-random digitally modulated signal. The performance of the link using both two tone analog modulation and pseudo random digital modulation are shown in Figure 26.

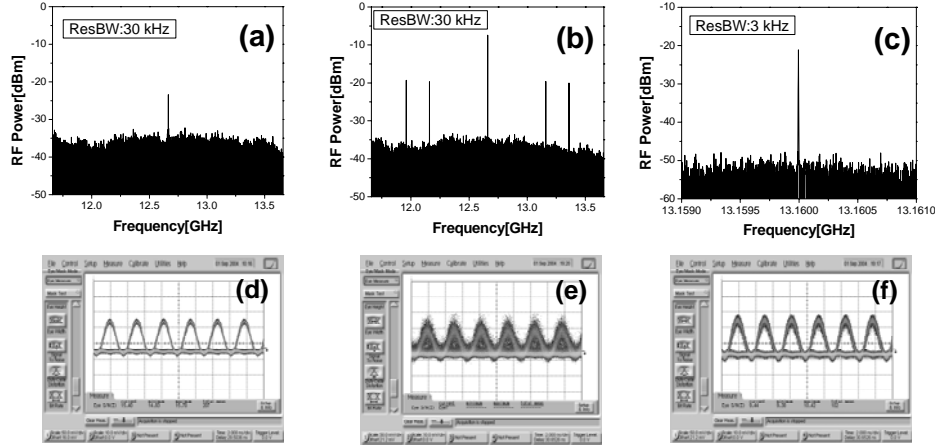


**Figure 26** Experimental results using the injection locked combs as a coherent receiver. (a-c) two-tone analog modulation. (d-e) 223-1 PRBS digital modulation

In Figure 26(a), is the coherently detected IF frequency at 12.66 GHz when the slave laser is not locked. The scan that is shown was chosen to illustrate a moment when the LO became randomly synchronized. Under normal unlocked conditions, there is a complete absence of a regenerated IF tone. Figure 26(b) shows the coherently detected IF and the associated two-tone modulated signals, under the conditions of robust injection locking. Note the strong recovery of the IF as well as the detected two-tone signal. Figure 26(c) shows a high resolution plot of one of the analog tones after filtering through a high Q microwave filter, in order to obtain information on the dynamic range of the link for the current operating parameters. In this case, a dynamic range of 60 dB/Hz was obtained and was limited by the optical power of the individual recovered optical frequency comb used in the coherent detection process [38].

Figure 26(d-f), shows the performance of the coherent receiver for pseudo random digital modulation. Figure 26(d) shows the back to back eye diagram for the case of using a single longitudinal mode from master laser and directly detecting pseudo-random digital modulation. The modulation rate was chosen as 316.5 MHz, with a  $2^{23}-1$  PSRB bit pattern. Figure 26(e) shows the performance of the coherent detection scheme, where a single longitudinal mode from the passive modelocked laser is used as a local oscillator to heterodyne detect the modulated carrier. The intermediate frequency is 6.33 GHz suggesting that 20 cycles of the intermediate frequency can be integrated to denote logical ones and zeros. In this case, the slave laser is not injection locked and hence, an envelope of the PSRB data is detected, with a closed eye. Figure 26(f) shows the



detected eye diagram when the slave laser is under injection locked conditions. The opened, well defined eye diagram, and its associated Q, implies error free operation ( $\text{BER} \sim 10^{-9}$ ) for a received power of  $\sim -16$  dBm and the conditions used in this experiment.

## **Conclusions**

Optical frequency combs generated from modelocked lasers have been shown to be ideal optical sinusoids for a variety of coherent signal processing applications, specifically for both optical and RF arbitrary waveform generation, and for coherent receiver architectures. Key in these applications is the need for the optical frequency comb generation (and regeneration) to be robust and stable. The use of the optical frequency combs to generate arbitrary sinusoids, RF bursts, and RF chirps has been demonstrated. The time-domain interleaving concept has also been proposed as a method to minimize undesirable optical and RF spurs in the synthesized waveform spectrum due to phase resetting limitations to ultimately realize endless operation at rates equal to the comb spacing, or pulse repetition rate of the modelocked laser. The optical frequency comb set has also been shown to be suitable for DWDM communication links using either direct detection or coherent detection where a second injection locked optical comb source is used for the receiver local oscillators. Future work in integrating filter technology with stabilized optical frequency comb sources will assist in suppressing the detrimental environmental effects that cause path length changes in the frequency multiplexing and demultiplexing stages. It is anticipated that as better integrated filter technology and ease of packaging and stabilizing optical frequency combs becomes available, optical coherent signal processing will become a mainstay in optical communications and signal processing applications.

## **Recommendations**

A frequency domain based architecture is described and discussed in this report for realizing RF and optical arbitrary waveform generators using optical frequency combs as an orthogonal basis set. The resulting arbitrary waveforms have the potential to possess a very high spur free dynamic range. Key to this high degree of fidelity is the need to realize endless phase modulation. The proposed approach achieves this by 'time domain interleaving' waveform segments to generate continuous arbitrary signals without signal signatures relating to phase modulators being reset. Future research should be related to further improvement in the time interleaving approach, as well as integration of the independent optoelectronic components, e.g., filtering/channelizing technologies and modulator technologies. An increase in the output optical power of the comb source as well as the power handling requirements of photodetectors would also be warranted.

## **References**

- [1] K. Nosu, "Advanced coherent lightwave technologies," *IEEE Commun. Magn.*, vol. 26, no. 2, pp. 15-21, Feb. 1988.
- [2] R. Linke and A. H. Gnauck, "High-capacity coherent lightwave systems," *J. Lightwave Technol.*, vol. 6, no. 11, pp. 1750-1769, Nov. 1988.
- [3] S. Etemad, P. Toliver, R. Menendez, J. Young, T. Banwell, S. Gail, J. Jackel, P. Delfyett, C. Price, T. Turpin, "Spectrally efficient optical CDMA using coherent phase-frequency coding", *IEEE Photon. Tech. Lett.*, Vol. 17, No. 4, 929-931, (2005).
- [4] A. J. Seeds, "Microwave photonics," *IEEE Trans. Microwave Theory Tech.* vol. 50, pp. 877-887, 2002.
- [5] A. M. Weiner, "Femtosecond pulse shaping using spatial light modulators", *Rev. Sci. Instr.*, vol. 71, no. 5, 1929-1960, (2000).
- [6] A. S. Bhushan, P. Kelkar and B. Jalali, "30 Gsamples/s time-stretch analog-to-digital converter," *Electr. Lett.* vol. 36, no. 18, pp. 1526-7, Aug. 2000.
- [7] T. Yilmaz, C. DePriest, T. Turpin, J. Abeles, P. J. Delfyett, "Toward a photonic arbitrary waveform generator using a modelocked external cavity semiconductor laser", *IEEE Photon. Tech. Lett.*, vol. 14, pp. 1608-1610, (2002).
- [8] B. Jalali, P. Kelkar, V. Saxena, "Photonic arbitrary waveform generator," in *2001 IEEE/LEOS Annual Meeting Conference Proceedings*, 2001, pp. 253-254.
- [9] Z. Jiang, D. S. Seo, D. E. Leiard, A. M. Weiner, "Spectral line-by-line pulse shaping", *Opt. Lett.*, Vol. 30, No. 12, pp. 1557-1559, (2005).
- [10] D. J. Jones, "Carrier-Envelope Phase Control of Femtosecond Mode-Locked Lasers and Direct Optical Frequency Synthesis," *Science*, vol. 288, Issue 5466, pp. 635-9, 2000.
- [11] S. T. Cundiff, "Phase stabilization of ultrashort optical pulses", *J. Phys. D*, vol. 35, no. 8, R43-R59, (2002).

- [12] R. K. Shelton, L.-S. Ma, H. C. Kapteyn, M. M. Murnane, J. L. Hall and J. Ye, "Phase-coherent optical pulse synthesis from separate femtoseconds lasers," *Science* vol. 293, Issue 5533, pp. 1286-9, 2001.
- [13] S. Stearns, Digital Signal Analysis, Hayden Book Co. (1975).
- [14] L. Cohen, Time – Frequency Analysis, Prentice Hall, (1995)
- [15] E. Frumker, E. Tal, Y. Silberberg, D. Majer, "Femtosecond pulse shape modulation at nanosecond rates" *Opt. Lett.*, Vol. 30, No. 20 2796-2798 (2005).
- [16] L. M. Johnson and C. M. Cox, "Serrodyne Optical Frequency Translation with High Sideband Suppression," *J. Lightw. Technol.*, vol. 6, no. 1, pp.109-112, Jan. 1998.
- [17] C. Laskoskie, H. Hung, T. El-Wailly, and C. L. Chang, "Ti-LiNbO<sub>3</sub> Waveguide Serrodyne Modulator with Ultrahigh Sideband Suppression for Fiber Optic Gyroscopes," *J. Lightw. Technol.*, vol. 7, no. 4, pp. 600-606, Apr. 1989.
- [18] M. Shen and R. A. Minasian, "Serrodyne optical frequency translation using photonics-based waveforms," *Electron. Lett.*, vol. 40, no. 24, pp. 1545-1547, Nov. 2004.
- [19] S. Ozharar, S. Gee, F. Quinlan, and P. J. Delfyett, "Heterodyne Serrodyne with High Sideband Suppression via Time Division Multiplexing for Arbitrary Waveform Generation," in *Proc. SPIE Int. Soc. Opt. Eng.* Vol. 5814, pp. 79-83, 2005.
- [20] G. T. Harvey and L. F. Mollenauer, "Harmonically mode-locked fiber ring laser with an internal Fabry-Perot stabilizer for soliton transmission," *Opt. Lett.* vol. 18, no. 2, pp. 107-9, 1993.
- [21] C. M. DePriest, T. Yilmaz, P. J. Delfyett, Jr., S. Etemad, A. Braun, J. Abeles, "Ultralow noise and supermode suppression in an actively mode-locked external-cavity semiconductor diode ring laser," *Optics Letters*, Vol. 27, No. 9, 719-721, (2002).
- [22] S. Gee, F. Quinlan, S. Ozharar, P. J. Delfyett, "Simultaneous optical comb frequency stabilization and super mode noise suppression of harmonically modelocked semiconductor ring laser using an intracavity etalon", , *IEEE Photonics Technology Letters* Vol. 17, No. 1, 199-201, (2005).

- [23] R. W. Drever, P., J. L. Hall, F. V. Kowalski, J. Hough, G. M. Ford, A. J. Munley and H. Ward, "Laser phase and frequency stabilization using an optical resonator," *Appl. Phys. B* vol. 31, issue 2, pp. 97-105, 1983.
- [24] T. Yilmaz, C. M. DePriest, A. Braun, J. Abeles, and P. J. Delfyett, Jr., "Residual phase noise and longitudinal mode linewidth measurements of hybridly modelocked external linear cavity semiconductor laser," *Optics Lett.*, vol. 27, 872-874, 2002.
- [25] T. Yilmaz, C. M. DePriest, and P. J. Delfyett, Jr., "Complete noise characterization of an external cavity semiconductor laser hybridly modelocked at 10 GHz," *Electron. Lett.*, vol. 37, pp. 1338-1339, 2001.
- [26] M. Shirasaki, "Large angular dispersion by a virtually imaged phased array and its application to a wavelength demultiplexer," *Opt. Lett.*, pp. 366-367, Vol. 21, No. 5, 1996.
- [27] M. Shirasaki, A. N. Akhter, and C. Lin, "Virtually Imaged Phased Array with Graded Reflectivity," *IEEE Photon. Technol. Lett.*, vol.11, no. 11, pp.1443-1445, Nov. 1999.
- [28] X. Shijun, A.M. Weiner, C. Lin, "Experimental and theoretical study of hyperfine WDM demultiplexer performance using the virtually imaged phased-array (VIPA)," *J. Lightwave Technol.*, vol. 23, pp. 1456 - 1467, 2005.
- [29] B.E. Little and S.T. Chu, "Toward very large-scale integrated photonics," *Optics & Photonics News*, pp24-29, Nov. 2000.
- [30] S. Ozharar, F. Quinlan, S. Gee, and Peter J. Delfyett, "Demonstration of endless phase modulation for arbitrary waveform generation", *IEEE Photon. Tech. Lett.*, Volume 17, Issue 12, pp. 2739 – 2741, Dec (2005).
- [31] K. Kikuchi and K. Katoh, "Optical heterodyne receiver for selecting densely frequency division multiplexed signals," *Electron. Lett.* vol. 38, no. 6, pp. 283-284, Mar. 2002
- [32] T. Kuri and K. Kiayama, "Optical heterodyne detection for 60GHz-band radio-on-fiber systems," *J. Commun. Research Laboratory*, vol. 49, no. 1, pp. 45-56, 2002.

- [33]N. Ohkawa, T. Sugie, and Y. Hayashi, “A highly sensitive balanced receiver for 2.5Gb/s heterodyne detection systems,” *IEEE Photon. Technol. Lett.*, vol. 3, no. 4, pp. 375-377, Apr. 1991.
- [34]B. K. Mathason and P. J. Delfyett, “Pulsed injection locking dynamics of passively mode-locked external-cavity semiconductor laser systems for all-optical clock recovery,” *J. Lightwave Tech.*, vol. 18, no. 8, pp.1111-1120, Aug. 2000.
- [35]K. Kikuchi, C.-E Zah, T. P. Lee, ‘Amplitude-modulation sideband injection locking characteristics of semiconductor lasers and their application’, *J. Lightwave Technol.*, **6**, pp. 1821-1830, (1988).
- [36]Z. Ahmed, H. F. Liu, D. Novak, Y. Ogawa, M. D. Pelusi, and D. Y. Kim, “Locking Characteristics of a passively mode-locked monolithic DBR laser stabilized by optical injection,” *IEEE Photon. Technol. Lett.*, vol. 8, no. 1, pp. 37-39, Jan. 1996.
- [37]W. Lee, and P. J. Delfyett, “Dual mode injection locking of two independent modelocked semiconductor lasers ,” *Electron. Lett., IEE*, Vol. 40, No. 19, pp 1182-1183, (2004).
- [38]W. Lee, M. Mielke, S. Etemad, P. J. Delfyett, “Subgigahertz channel filtering by optical heterodyne detection using a single axial mode from an injection-locked passively mode-locked semiconductor laser”, *IEEE Photonics Technology Letters*, Volume: 16 , Issue: 8 , 1945 – 1947 (2004).